Pyroelectric current measurements on $PbZr_{0.2}Ti_{0.8}O_3$ epitaxial layers

B. Bhatia,[1] J. Karthik,[2] T. Tong,[2] David G. Cahill,[1,2] L. W. Martin,[2] and W. P. King[1,2,a)]
[1]*Department of Mechanical Science and Engineering, University of Illinois Urbana-Champaign, Urbana, Illinois 61801, USA*
[2]*Department of Materials Science and Engineering and Materials Research Laboratory, University of Illinois Urbana-Champaign, Urbana, Illinois 61801, USA*

(Received 23 August 2012; accepted 17 October 2012; published online 21 November 2012)

We report pyroelectric current measurements on 150 nm thick $PbZr_{0.2}Ti_{0.8}O_3$ (PZT) epitaxial films using frequency-domain thermal measurements over the range 0.02 Hz–1.3 MHz. The measured pyroelectric currents are proportional to the rate of temperature change, from $\sim 10^{-5}$ A/m^2 to $\sim 10^3$ A/m^2 over the range 10^{-2} to 10^6 K/s. The film temperature oscillation is controlled using either a hotplate, microfabricated heater, or modulated laser, and the pyroelectric current is measured from a microelectrode fabricated onto the film. The measured pyroelectric coefficient of the PZT films is nearly constant across the entire frequency range at ≈ -200 μC/m^{2}K. © *2012 American Institute of Physics*. [http://dx.doi.org/10.1063/1.4766271]

I. INTRODUCTION

Pyroelectricity, the temperature dependence of spontaneous polarization,[1] enables a variety of devices[2–4] that utilize the pyroelectric current generated by temperature fluctuations. Pyroelectric materials are used in applications such as thermal imaging, radiometry, environmental monitoring, and gas analysis, all of which rely on bulk ferroelectric materials. However, future nanoscale electronic and energy conversion devices will increasingly require thin films. Challenges facing thin-film ferroelectrics include their susceptibility to size- and strain-induced effects. Over the last few decades, thin-film epitaxy has developed dramatically and it is now possible to synthesize ferroelectric thin films with control over film composition, epitaxial strain, electrical boundary conditions, and thickness.[5–7] These synthesis capabilities have been instrumental in developing an understanding of the dielectric, piezoelectric, and ferroelectric responses of thin-film materials. However, understanding the pyroelectric response of thin films remains a challenge, owing to pinhole defects and trapped charges in these films.[8] The lack of understanding of pyroelectric properties in thin films has limited the development of pyroelectric materials and new devices based on these materials. Techniques to measure pyroelectric currents and the pyroelectric coefficient of thin films are thus urgently needed in order to enable new applications of pyroelectric thin films.[8–10]

Conventional techniques to characterize pyroelectric response are based on heating by a laser[11] or simply placing the material on a hotplate or in a furnace.[12] These techniques were developed for bulk ceramics or single crystals, and are adequate for large samples. The techniques using bulk sample heating have had limited success in their application to thin films due to defects in the thin films as well as thermally activated trapped charges.[8,13–15] It is possible to achieve higher rates of temperature change using, for example, laser heating. Dynamic techniques that rapidly modulate the sample temperature allow for the measurement of continuous pyroelectric current.[16,17] When the temperature change is due to continuous temperature oscillations at a single frequency, the pyroelectric current measurement accuracy can be higher than for temperature changes that are step changes, pulses, or ramps, since a periodic current can be conveniently measured using phase-sensitive detection with high signal-to-noise.[8,18] When the sample is periodically heated by a hotplate or thermoelectric element, the rate of temperature change is typically limited to $\sim$1 K/s. When the sample is periodically heated using laser intensity modulation, the temperature can oscillate in the range 10^3–10^6 K/s.[19,20] However, there is a lack of publications showing frequency-domain pyroelectric current measurements in the range 1–10^3 K/s.[21] Furthermore, there has been little work to compare pyroelectric properties across different measurement techniques. Comparison of pyroelectric measurements using independent techniques allows validation of the experimental results in the absence of any baseline measurements of thin film pyroelectric properties. It can be difficult, however, to compare pyroelectric property measurements across different techniques, since this comparison requires accurate measurements of the thermal properties of the pyroelectric thin film, which are in general not independently measured. Thus, there remains significant unmet need for pyroelectric property measurements on solid state thin films.

Here, we present frequency-domain measurements of pyroelectric currents from thin films of $PbZr_{0.2}Ti_{0.8}O_3$ (PZT). 150 nm thick PZT films were grown on $DyScO_3$ (DSO) (110) single crystal substrates with 20 nm $SrRuO_3$ (SRO) bottom electrodes via pulsed-laser deposition.[22] (See supplementary material for the details of film deposition and characterization.)[23] We independently measure the thermal properties of the pyroelectric thin films using time domain thermoreflectance,[24] allowing for accurate estimates of the temperature distribution within the sample. The pyroelectric current measurements use either bulk heating for low frequency periodic (LFP) measurements, microfabricated resistive heaters for 2ω measurements, or a chopped laser beam

a)Electronic mail: wpk@illinois.edu.

for laser intensity modulation (LIM) measurements. We measure the pyroelectric coefficient of the thin-film samples in three different frequency regimes: less than 1 Hz (LFP), from 10 Hz to 1 kHz (2ω), and above 100 kHz (LIM). We compare these techniques to each other and to the widely used direct method[12] for pyroelectric current measurement.

II. MEASUREMENTS

A. Direct and low frequency periodic measurements

Figure 1 illustrates pyroelectric measurement using the direct[12] and LFP methods.[16,17] The sample consisted of 100 μm diameter axisymmetric capacitors with a 80 nm SRO/150 nm PZT/20 nm SRO device structure produced via an MgO hard-mask process [Figure 1(a)].[25] A current amplifier mounted close to the sample measured the current from the top SRO electrode during heating, while the sample was mounted in a dark faraday cage to reduce environmental noise. Figure 1(b) shows the direct measurement temperature and current profiles. We increased the temperature at a constant rate from 300 to 350 K in 300 s, then held the temperature at 350 K for 100 s before the heater was turned off such that the sample could cool. A linear temperature ramp should result in a constant, non-zero pyroelectric current $i_p = pA(dT/dt)$, where p is the pyroelectric coefficient, A is the area of the electrode, and dT/dt is the rate of change of temperature with time, in this case 0.16 K/s. The measured current is, however, not constant with a constant temperature rate, and there is non-zero current when the temperature is constant. These data illustrate the difficulty in measuring pyroelectric response using conventional direct measurement techniques. Although some of the current is pyroelectric, there are non-pyroelectric currents, most likely resulting from thermally stimulated currents that result from temperature-induced releasing of trapped charges.[13–16,26] This effect is a particular problem for thin films, where the density of trapped charges can be larger than in bulk samples.

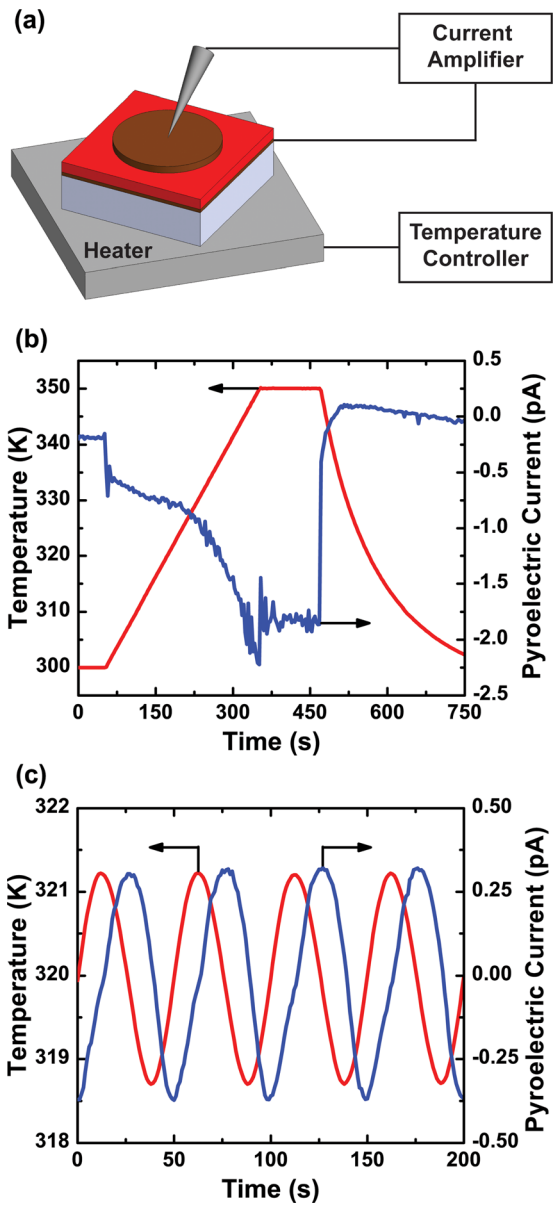

FIG. 1. (a) Setup for pyroelectric measurement using the (b) direct and (c) LFP method. The direct method uses a linear temperature ramp. The LFP method uses low frequency sinusoidal temperature oscillation. Resulting pyroelectric current is shown. The direct measurement showed contribution from non-pyroelectric current. The LFP measurement used an oscillatory temperature with ≈1.25 K amplitude and 0.02 Hz frequency. Amplitude of resulting pyroelectric current was less than 1 pA.

Figure 1(c) shows the temperature and current for pyroelectric measurement using the LFP method. A sinusoidal temperature oscillation, with a background temperature of 320 K (T_b) and 1.25 K (T_0) amplitude, was applied to the sample at 0.02 Hz ($\omega = 0.125$ rad/s). The sample temperature is $T = T_b + T_0 \sin(\omega t)$ and the theoretical pyroelectric current is $i_p = pAT_0\omega \cos(\omega t)$. Thus, the pyroelectric current should be phase-shifted from the temperature oscillations by 90°. The measured pyroelectric current was fitted to a sine function, $i_0 \sin(\omega t + \phi)$, to extract the magnitude, i_0, and phase of the pyroelectric current with respect to the temperature oscillation, ϕ. The pyroelectric coefficient was then obtained by considering the out-of-phase component of the measured current as $p = i_0 \sin(\phi)/AT_0\omega$. While the LFP technique works reasonably well for this thin film, precise control of the sample temperature is difficult and the measurement must be performed at low heating frequencies to ensure thermal equilibrium, which results in a low pyroelectric current and signal-to-noise ratio. One advantage of these direct measurements is that the sample is in thermal equilibrium, and so the temperature can be estimated without detailed knowledge of the pyroelectric thin film thermal properties.

B. 2ω measurements

Figure 2(a) shows the measurement setup for pyroelectric measurement using the 2ω method. Periodic electrical excitation of a 20 μm wide platinum strip with chromium adhesion layer at frequency ω produces a temperature oscillation at a frequency 2ω.[27] This temperature oscillation generates a pyroelectric current that is measured using the current input (10^6 V/A gain) of a lock-in amplifier.[28] The SiO_2 layer deposited on the pyroelectric film ensures that the external electric field across the pyroelectric film is negligible and does not interfere with the pyroelectric

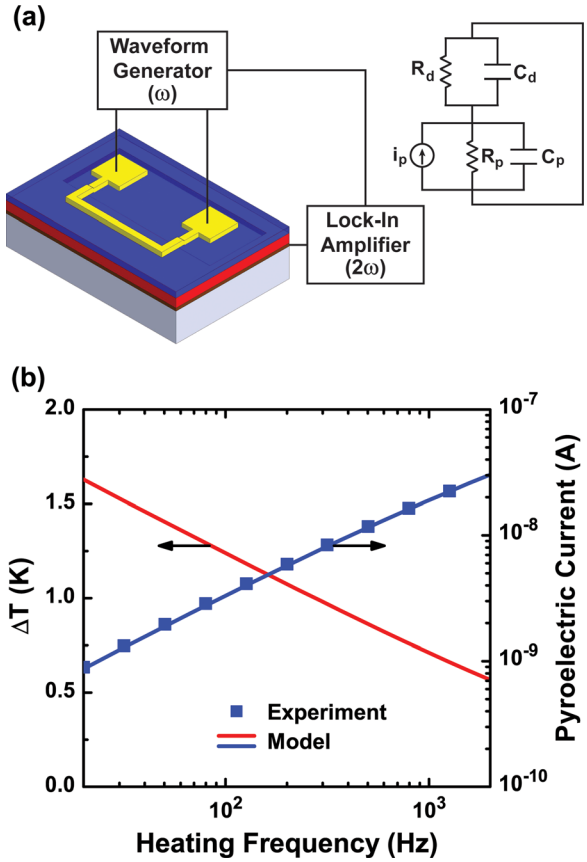

FIG. 2. (a) Setup for pyroelectric measurement using the 2ω method. A lock-in amplifier measures the pyroelectric current at frequency 2ω generated due to a temperature oscillation caused by electrical excitation at frequency ω. The pyroelectric layer is modeled as a current source with intrinsic resistance and capacitance as shown in the equivalent circuit (top-right). (b) Magnitude of pyroelectric current and temperature oscillation amplitude plotted as a function of heating frequency. A constant pyroelectric coefficient was used to fit the theoretical model and experiment. Data are shown for 4.26 W/m input power per unit heating length.

response of the thin film. We verified that the resulting signal was due to periodic heating of the metal strip and not a voltage-based artifact by comparing the 2ω current measured at different strip biases but with the same heating power using a series resistor before or after the metal strip. (See supplementary material for device design, fabrication, and characterization.)[23]

The equivalent circuit shown in the top-right of Figure 2(a) relates the measured 2ω current to the pyroelectric current. The pyroelectric layer is modeled as a current source in parallel with a dielectric, which is a resistor and capacitor in parallel.[29,30] The SiO_2 passivation layer is represented by an equivalent resistance and capacitance. The pyroelectric current, $i_{p,2\omega}$, is evaluated from the measured 2ω current, $i_{2\omega}$, as

$$i_{p,2\omega} = i_{2\omega}\left(\frac{Z_p}{Z_p + Z_d}\right)^{-1}, \tag{1}$$

where $Z_p = \frac{R_p}{1+j(2\omega)R_pC_p}$ and $Z_d = \frac{R_d}{1+j(2\omega)R_dC_d}$. The resistance ($R$), capacitance ($C$), and electrical impedance (Z) of the pyroelectric (PZT) and dielectric (SiO_2) films are indicated by the subscripts p and d, respectively. The resistivity and dielectric constant of the PZT and SiO_2 films were measured independently to evaluate intrinsic resistance and capacitance (see supplementary material for details[23]).

Since the heating frequency is low (<2 kHz) and the thermal penetration depth is much larger than the film thicknesses, the heat diffusion is one-dimensional in the radial direction. We use this model to relate electrical power input with the resulting temperature oscillations as in the 3ω method.[31,32] The frequency-dependent temperature oscillations of the semi-infinite substrate due to the line heat source of width $2b$ and length l is given by[33]

$$\Delta T_s = \frac{P}{l\pi\Lambda_s}\int_0^\infty \frac{\sin^2(kb)}{(kb)^2(k^2+q^2)^{1/2}}dk, \tag{2}$$

where $q^{-1} = (D/j2\omega)^{1/2}$ is the thermal penetration depth, $j = \sqrt{-1}$, P is the input power, D is the thermal diffusivity, and Λ_s is the substrate thermal conductivity. The thin films between the metal line and substrate each add a frequency-independent temperature oscillation given by[34]

$$\Delta T_f = \frac{P}{l\Lambda_f}\frac{t}{2b}, \tag{3}$$

where t is the film thickness and Λ_f is the film thermal conductivity, which was measured using time domain thermoreflectance.[24] The temperature oscillation of the PZT film can then be evaluated by adding the contributions from the substrate, SRO layer and half the PZT layer, $\Delta T = \Delta T_s + \Delta T_{f(SRO)} + \frac{1}{2}\Delta T_{f(PZT)}$. The pyroelectric current, $i_p = pA(dT/dt)$, can thus be written as a function of temperature oscillation ΔT at a frequency 2ω as

$$i_{p,2\omega} = jpA(2\omega)\Delta T. \tag{4}$$

Figure 2(b) shows the amplitude of the temperature oscillation and the magnitude of measured pyroelectric current measured as a function of heating frequency for an input heating power of 4.26 W per unit length (m). The solid lines show the predicted amplitude of the temperature oscillation [Eqs. (2) and (3)] and the magnitude of the pyroelectric current [Eq. (4)]. The symbols show the pyroelectric current obtained from the 2ω current measurement [Eq. (1)]. The pyroelectric coefficient is the only free parameter and is obtained by fitting the model to the measured data. Pyroelectric current magnitude of >1 nA was measured in comparison to <1 pA for the LFP method.

C. Laser intensity modulation measurements

Pyroelectric characterization at an even higher frequency range is possible using laser diagnostics. Figure 3(a) shows the measurement setup used for pyroelectric measurement using a modulated laser as a local heat source. Previous publications reported the pyroelectric response of thin films using laser intensity modulation but lacked accurate thermal property values required to fully analyze the data.[11,19,20] Improvements in laser-based diagnostics now enable more accurate measurements.[24] Our LIM method probes the

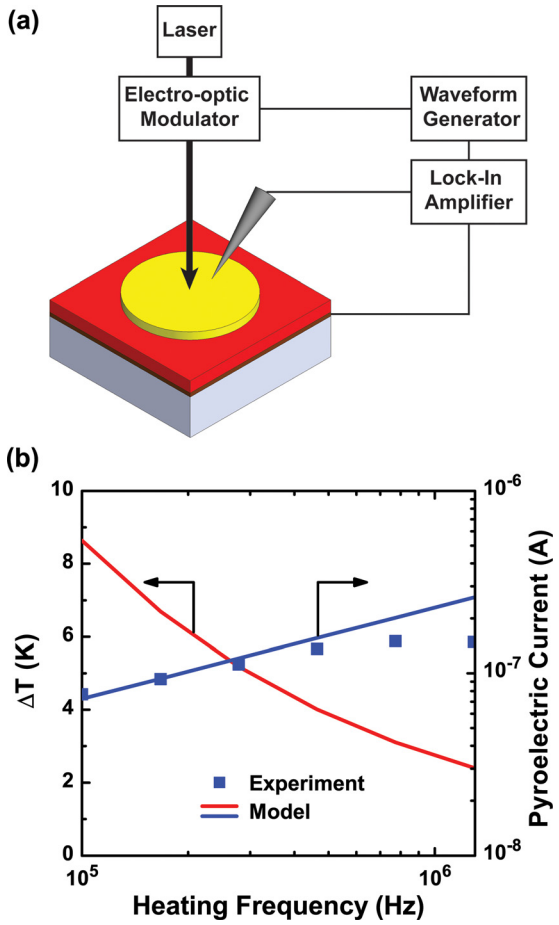

FIG. 3. (a) Setup for LIM based pyroelectric measurement. The laser power absorbed by the sample was 1.3 mW and the $1/e^2$ radius of the beam was 4.7 μm. An RF lock-in amplifier measures the pyroelectric current at the laser modulation frequency. (b) Magnitude of pyroelectric current and temperature oscillation amplitude as a function of modulation frequency. A constant pyroelectric coefficient was used to fit the theoretical model and experiment.

pyroelectric response of the thin film using a Ti:sapphire laser oscillator with a repetition rate of 80 MHz. Using an electro-optical modulator, the laser beam was modulated from 100 kHz–1.3 MHz and the pyroelectric response was probed with a spatial resolution of $<10\,\mu$m. Measurements were done on capacitors consisting of 180 nm thick PZT, with SRO bottom electrode and 20 μm wide, 1.4 mm long platinum top electrodes with a chromium adhesion layer. The platinum top electrode (optical absorption coefficient = 0.29, at a wavelength of 785 nm) absorbed the laser power to raise the temperature. The periodic modulation of the laser beam causes periodic temperature oscillation within the film. This temperature oscillation generates a pyroelectric current at the modulation frequency which is measured using a lock-in amplifier. For a heating frequency >100 kHz, the thermal penetration depth is small compared to the $1/e^2$ radius of the laser beam ($w_0 = 4.7\,\mu$m). Hence, the temperature oscillation amplitude of the substrate is given by a one-dimensional heat flow model with a uniform heat flux $P/(\pi w_0^2)$,[24]

$$\Delta T_s = \frac{P}{\pi w_0^2 \sqrt{j\omega \Lambda_s C_s}}, \tag{5}$$

where C_s is the volumetric heat capacity of the substrate. The temperature oscillation of the PZT film can be evaluated by including the contributions from the SRO layer and half the PZT layer using Eq. (3), $\Delta T = \Delta T_s + \Delta T_{f(SRO)} + {}^1/_2\,\Delta T_{f(PZT)}$. The resulting pyroelectric current is

$$i_p = jp(\pi w_0^2)\omega \Delta T. \tag{6}$$

Figure 3(b) shows the amplitude of temperature oscillation and pyroelectric current as a function of the laser modulation frequency. The laser power absorbed by the sample was 1.3 mW. Temperature oscillation amplitude was estimated using Eqs. (3) and (5). The model [Eq. (6)] was fitted to the measured pyroelectric current to estimate the pyroelectric coefficient of the PZT thin film. One value of the pyroelectric coefficient was used in the model for fitting across the entire heating frequency range. At high frequencies, the capacitive reactance of the sample decreases significantly. Since the model does not account for the sample capacitance, we observe a mismatch between the measured and predicted pyroelectric current at high heating frequencies. This LIM method allowed quantitative characterization of sub-micron epitaxial pyroelectric layers at high frequency with a spatial resolution $<10\,\mu$m.

III. RESULTS AND DISCUSSION

Our measurements span heating frequencies from 0.02 Hz to 1.3 MHz. Figure 4(a) shows the magnitude of the pyroelectric current per unit heating area as a function of time rate of change of temperature for each of the three methods. The error bars correspond to standard deviation from measurements done on multiple devices across different samples. Pyroelectric current density is directly proportional to the rate of change of temperature with time dT/dt. The pyroelectric current density increases by eight orders of magnitude as the time rate of change of temperature varies from 0.018 K/s for the LFP method to 3.1×10^6 K/s using the LIM method.

Figure 4(b) compares the phase difference between the measured pyroelectric current and estimated temperature oscillation as a function of rate of heating for the three methods. The true pyroelectric current is phase-shifted from the temperature oscillations by 90°.[16] However, a non-90° phase-shift is commonly observed due to thermally stimulated current and other artifacts. Our measurements show that the phase difference is nearly 90° for the 2ω method, whereas a noticeable deviation is observed for the LFP measurements. We believe that this deviation in phase difference is due to the release of trapped charges due to bulk heating of the sample in the LFP technique that occurs in phase with the temperature change. For the LIM method, sample capacitance causes a phase shift between the phase of heating (laser modulation) and the phase of the measured pyroelectric current. This is not accounted for in our simplified model and hence the discrepancy in the phase data at high heating frequencies (see supplementary material for details of the phase difference calculation[23]).

Figure 5 shows the measured pyroelectric coefficients of PZT 20/80 thin films on DSO substrate as a function of

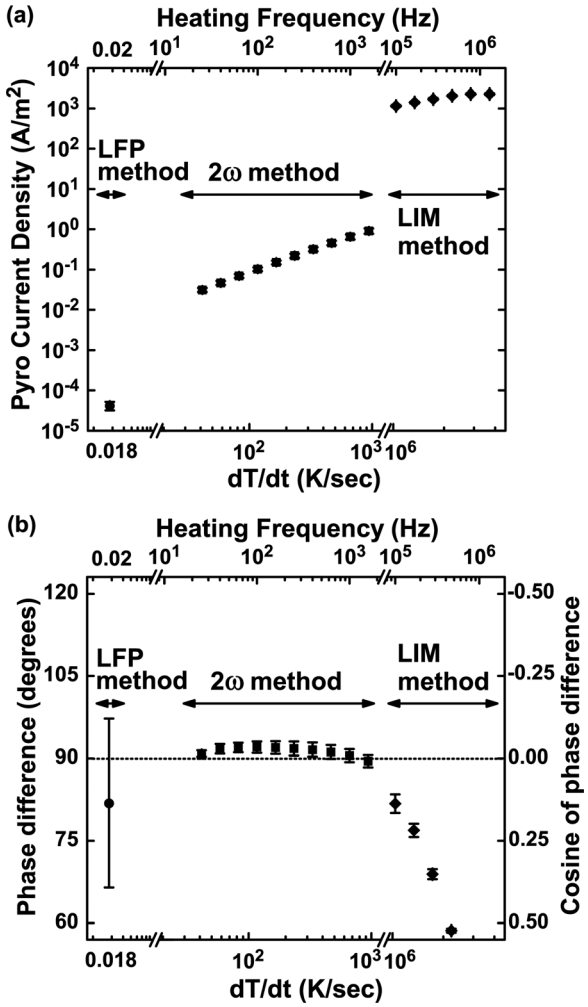

FIG. 4. (a) Magnitude of pyroelectric current density and (b) phase difference between pyroelectric current and temperature oscillation plotted as a function of rate of temperature change for LFP, 2ω, and LIM measurements.

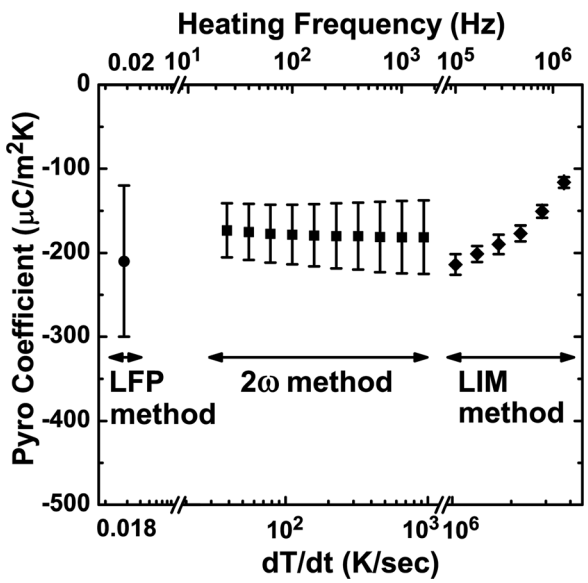

FIG. 5. Pyroelectric coefficient of $PbZr_{0.2}Ti_{0.8}O_3$ thin films measured using the LFP, 2ω, and LIM methods plotted as a function of the rate of temperature change. The pyroelectric coefficient is nearly constant for the heating frequency range of 0.02 Hz–1.3 MHz.

heating rate. The figure shows results from the LFP, 2ω, and LIM measurements, but it was not possible to estimate the pyroelectric coefficient using the direct method because of the significant thermally stimulated current contribution. Unlike the model results shown in Figures 2(b) and 3(b), where a single pyroelectric coefficient was used in the model across the entire heating frequency range, pyroelectric coefficients were estimated by fitting the theoretical model to the measured pyroelectric current at each heating frequency. The measured pyroelectric coefficient is nearly constant at $\approx -200\ \mu C/m^2K$ across a large range of heating rates, which is close to $-180\ \mu C/m^2K$ reported for poled PZT 20/80 films deposited via spin coating.[35] The pyroelectric response is essentially unchanged up to 1 MHz, which is consistent with other frequency-dependent measurements reported in the literature.[36,37] The observed reduction in the pyroelectric coefficient magnitude near 1 MHz heating frequency can be attributed to capacitive effects not included in the modeling. While there may be thermomechanical-induced strains in the pyroelectric layer, any currents generated by these strains are small relative to the pyroelectric currents observed here.

IV. SUMMARY

We have demonstrated three frequency-domain techniques for measuring pyroelectric currents from PZT thin films using temperature oscillations over the range 0.02 Hz to 1.3 MHz. Measurements using low frequency 1.25 K temperature oscillations produce pyroelectric current less than 1 pA which is below the noise floor of most measurement setups. Developed specifically for thin films, the 2ω method, proved more robust as it produced easily measurable pyroelectric current greater than 1 nA between 20 Hz-2 kHz heating frequencies. An even higher heating frequency regime was made accessible by using a laser-based method that resulted in pyroelectric currents of ~100 nA. These techniques enable the study of pyroelectric thin films, which could improve future nanoscale electronics and energy conversion devices using these films.

ACKNOWLEDGMENTS

The authors gratefully acknowledge the support of ONR N00014-10-1-0525.

[1]M. E. Lines and A. M. Glass, *Principles and Applications of Ferroelectrics and Related Materials* (Clarendon, Oxford, 1977).
[2]R. W. Whatmore, Rep. Prog. Phys. **49**(12), 1335 (1986).
[3]R. B. Olsen, D. A. Bruno, and J. M. Briscoe, J. Appl. Phys. **58**(12), 4709 (1985).
[4]A. Hadni, J. Phys. E: J. Sci. Instrum. **14**(11), 1233 (1981).
[5]M. Dawber, K. M. Rabe, and J. F. Scott, Rev. Mod. Phys. **77**(4), 1083 (2005).
[6]D. G. Schlom, L. Q. Chen, C. B. Eom, K. M. Rabe, S. K. Streiffer, and J. M. Triscone, Annu. Rev. Mater. Res. **37**, 589 (2007).
[7]L. W. Martin, Y. H. Chu, and R. Ramesh, Mater. Sci. Eng. R. **68**, 89 (2010).
[8]I. Lubomirsky and O. Stafsudd, Rev. Sci. Instrum. **83**(5), 051101 (2012).
[9]S. B. Lang, Phys. Today **58**(8), 31 (2005).
[10]J. F. Scott, Annu. Rev. Mater. Res. **41**, 229 (2011).
[11]A. G. Chynoweth, J. Appl. Phys. **27**(1), 78 (1956).
[12]R. L. Byer and C. B. Roundy, Ferroelectrics **3**, 333 (1972).

[13]H. Okino, Y. Toyoda, M. Shimizu, T. Horiuchi, T. Shiosaki, and K. Matsushige, Jpn. J. Appl. Phys. **37**, 5137 (1998).
[14]T. Nishida, M. Matsuoka, S. Okamura, and T. Shiosaki, H. Okino, Y. Toyoda, M. Shimizu, T. Horiuchi, T. Shiosaki, and K. Matsushige, Jpn. J. Appl. Phys. **42**, 5947 (2003).
[15]W. Liu and C. A. Randall, J. Am. Ceram. Soc. **91**(10), 3251 (2008).
[16]L. E. Garn and E. J. Sharp, J. Appl. Phys. **53**(12), 8974 (1982).
[17]E. J. Sharp and L. E. Garn, J. Appl. Phys. **53**(12), 8980 (1982).
[18]M. Daglish, Integr. Ferroelectr. **22**(1–4), 473 (1998).
[19]S. B. Lang and D. K. Dasgupta, J. Appl. Phys. **59**(6), 2151 (1986).
[20]S. B. Lang, Ferroelectrics **186**, 53 (1996).
[21]J. Defrutos and B. Jimenez, Ferroelectrics **109**, 101 (1990).
[22]J. Karthik, A. R. Damodaran, and L. W. Martin, Phys. Rev. Lett. **108**(16), 167601 (2012).
[23]See supplementary material at http://dx.doi.org/10.1063/1.4766271 for PZT film deposition, device design and fabrication for the 2 ω method, pyroelectric current and temperature oscillation amplitudes and phase difference, and modeling property values.
[24]D. G. Cahill, Rev. Sci. Instrum. **75**(12), 5119 (2004).
[25]J. Karthik, A. R. Damodaran, and L. W. Martin, Adv. Mater. **24**(12), 1610 (2012).
[26]W. Liu and C. A. Randall, J. Am. Ceram. Soc. **91**(10), 3245 (2008).
[27]N. O. Birge and S. R. Nagel, Rev. Sci. Instrum. **58**(8), 1464 (1987).
[28]B. Smith and C. Amon, J. Electron. Packag. **129**(4), 504 (2007).
[29]S. B. Lang and F. Steckel, Rev. Sci. Instrum. **36**(7), 929 (1965).
[30]G. A. Burdick and R. T. Arnold, J. Appl. Phys. **37**(8), 3223 (1966).
[31]D. G. Cahill, Rev. Sci. Instrum. **61**(2), 802 (1990).
[32]C. Dames and G. Chen, Rev. Sci. Instrum. **76**(12), 124902 (2005).
[33]D. G. Cahill, H. E. Fischer, T. Klitsner, E. T. Swartz, and R. O. Pohl, J. Vac. Sci. Technol. A **7**(3), 1259 (1989).
[34]D. G. Cahill, M. Katiyar, and J. R. Abelson, Phys. Rev. B **50**(9), 6077 (1994).
[35]N. M. Shorrocks, A. Patel, M. J. Walker, and A. D. Parsons, Microelectron. Eng. **29**(1–4), 59 (1995).
[36]S. Yablonskii, E. A. Soto-Bustamante, V. H. Trujillo-Rojo, and V. Sorokin, J. Appl. Phys. **104**(11), 114102 (2008).
[37]M. Dietze, J. Krause, C. H. Solterbeck, and M. Es-Souni, J. Appl. Phys. **101**(5), 054113 (2007).